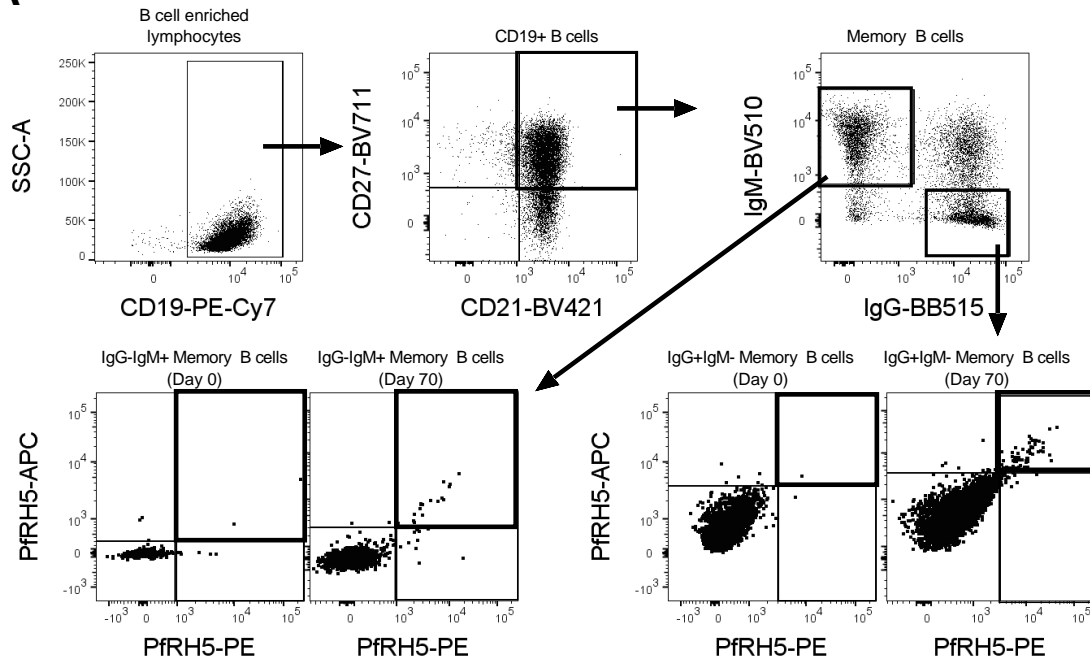
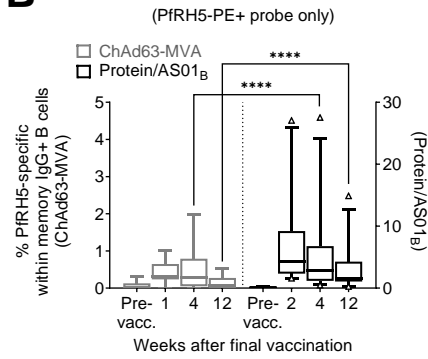
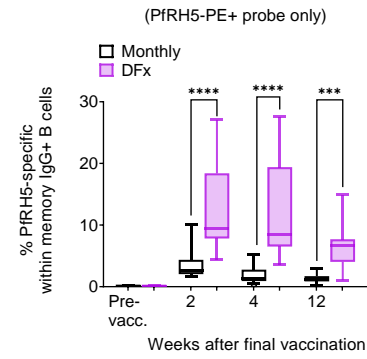
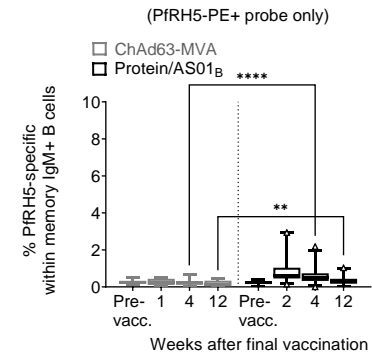


1 Supplemental Figures and Tables

A**B****C****D**

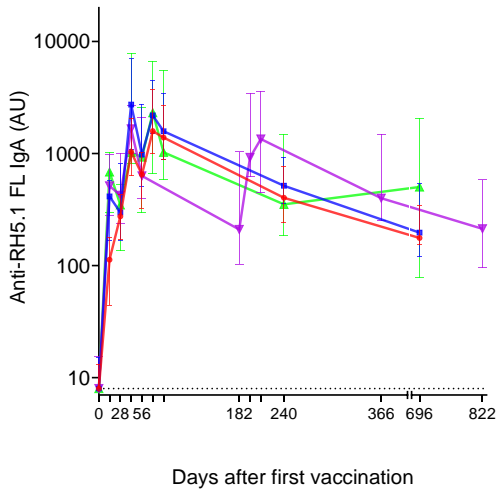
3 **Supplemental Figure 1. Gating strategies for defining PfrH5-specific B cells in flow cytometry-based assays.**

4 **Relates to Figures 1 and 4.**

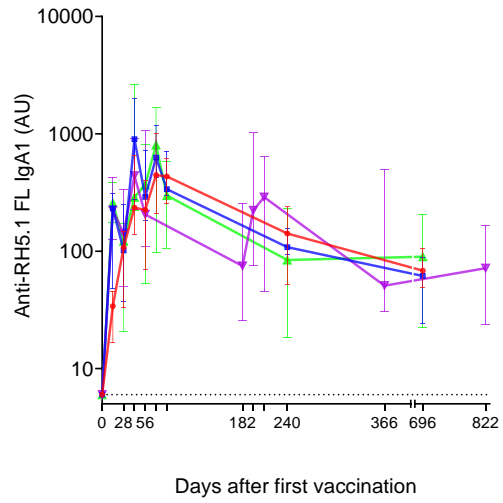
5 PBMC from pre-vaccination (Pre-vacc.), and 1-, 2-, 4-, and 12-weeks post final vaccination time points were enriched for B cells and then stained
6 with phenotypic markers and analysed by flow cytometry. **(A)** Gating strategy for PfrH5-specific IgG/ IgM CD19+ B cells within the live lymphocyte
7 population. For data in **Figure 1**, the panel included CD21/CD27 to define memory IgG+ B cells as CD19+CD21+CD27+IgG+IgM-. A more limited
8 panel was used for the single cell sorting as shown in **Figure 4**, to gate the wider CD19+ IgG+ B cell population (no CD21/CD27/IgM staining).
9 For both **Figure 1** and **Figure 4**, PfrH5-specific cells were defined by co-staining with monobiotinylated-PfrH5 conjugated to streptavidin-PE
10 and monobiotinylated-PfrH5 conjugated to streptavidin-APC (PfrH5-PE+PfrH5-APC+). Panels **(B-D)** show the frequencies of PfrH5-specific
11 mBCs when defined only on the basis of PfrH5-PE+. With this less stringent approach, frequencies of PfrH5-specific memory IgG+ B cells
12 (CD19+CD21+CD27+IgG+IgM-) were compared between **(B)** samples from a heterologous viral vector trial (ChAd63-MVA; ChAd63-PfrH5
13 prime, MVA-PfrH5 boost (1, 2)) and the protein/AS01_B trial (3), or **(C)** between monthly regimen vaccinees and DfX vaccinees within the
14 protein/AS01_B trial. Frequencies of PfrH5-specific memory IgM+ B cells (CD19+CD21+CD27+IgG-IgM+) were also compared using the PfrH5-
15 PE probe only **(D)**. **(B, D)** ChAd63-MVA/ protein/AS01_B: Pre-vacc. $n = 15/18$; 1-week post final vaccination $n=10/0$; 2-week $n=0/25$; 4-week
16 $n=15/29$; 12-week $n=13/25$. **(C)** Monthly / DfX within protein/AS01_B trial: Pre-vacc. $n=15/3$; 2-week $n=16/9$; 4-week $n=19/10$; 12-week $n=17/8$.
17 Comparisons were performed by Mann-Whitney tests. Central box lines indicate medians and whiskers denote 5th and 95th percentiles; samples
18 outside the 5-95th percentile range are shown as triangles. ** $p < 0.01$, **** $p < 0.0001$.

■ Monthly-low
 ■ Monthly-medium
 ■ DFx
 ■ Monthly-high

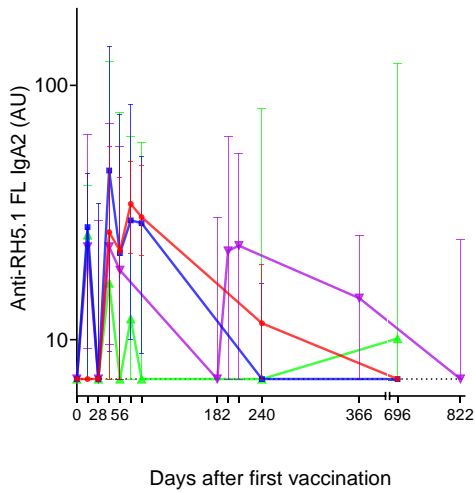
A



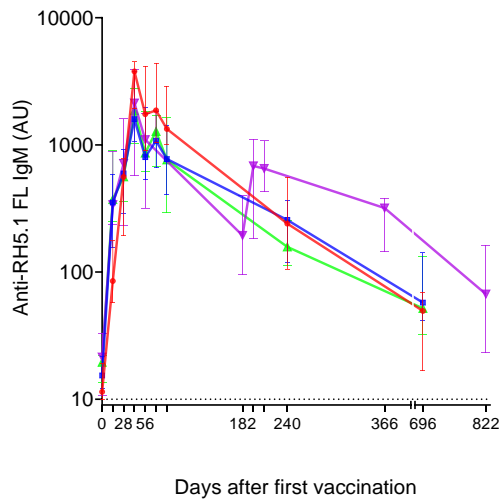
B



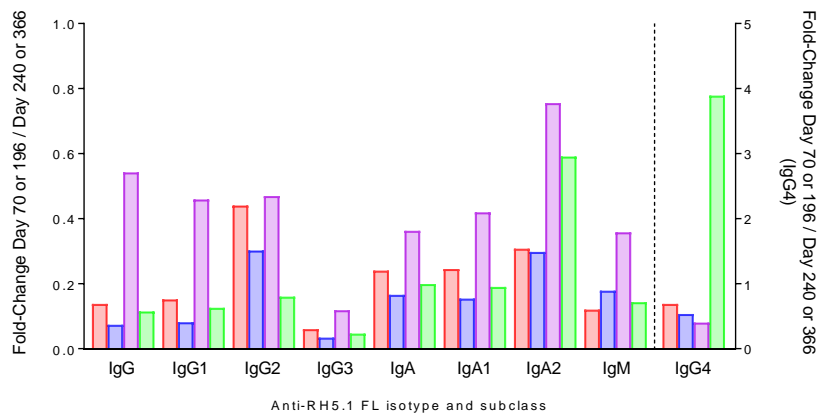
C



D



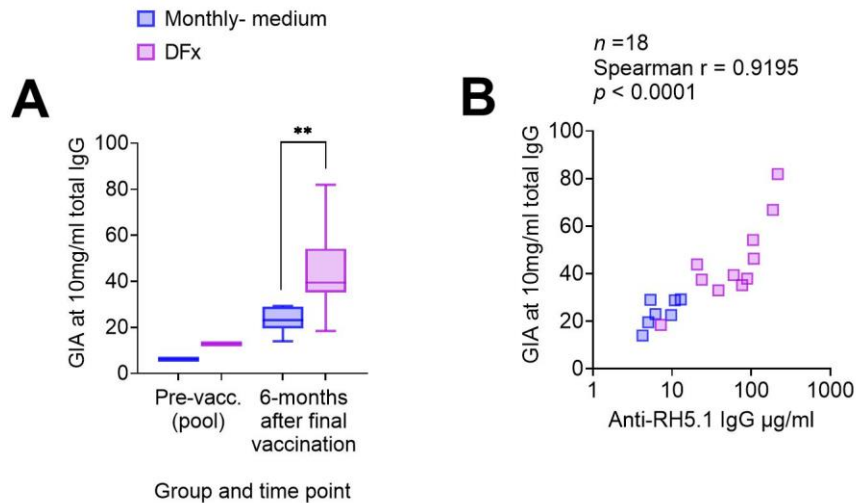
E



20 Supplemental Figure 2. Antigen-specific IgA and IgM post-vaccination kinetics
21 in Dfx and monthly dosing regimens.

22 **Relates to Figure 1.**

23 Serum anti-PfRH5.1 FL (full length RH5.1) Ig was assayed by standardised ELISA to report
24 (A) total IgA, (B) IgA1, (C) IgA2, and (D) IgM at key time points (Days 0, 14, 28, 42, 56/182,
25 70/196, 84/210, 240/366, 696/822). (E) Fold change in anti-PfRH5.1 FL Ig between 2-weeks
26 after final vaccination (Day 70 for monthly regimen vaccinees, and Day 196 for Dfx vaccinees)
27 and 6-months after final vaccination (Day 240, Day 366). Sample sizes for these ELISAs
28 varied by group and by time point. Monthly-low: $n=12$, except Day 696 ($n=9$). Monthly-medium:
29 $n=12$, except Days 240 ($n=11$) and 696 ($n=10$). Dfx: $n=12$, except Days 366 ($n=11$) and 822
30 ($n=7$). Monthly-high: $n=11$, except Days 70 ($n=9$), 240 ($n=10$) and 696 ($n=4$). Graphs show
31 medians and (for A-D) interquartile ranges.

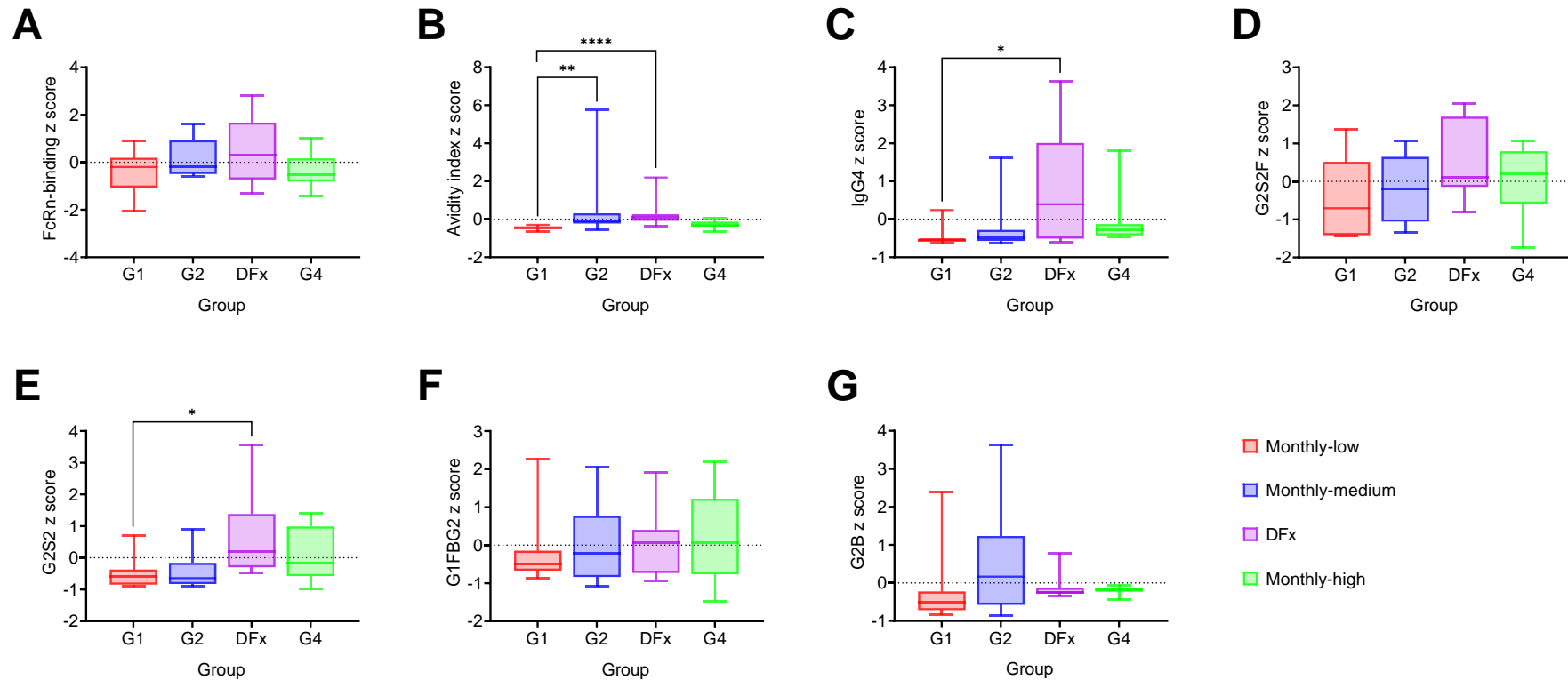


32

33 [Supplemental Figure 3. DFX anti-RH5.1 IgG 6-months after final vaccination](#)
 34 [correlates with in vitro parasite growth inhibition.](#)

35 **Relates to Figure 1.**

36 IgG purified from pooled pre-vaccination and individual post-vaccination samples was
 37 incubated with *Plasmodium falciparum*-infected red blood cells to determine parasite growth
 38 inhibition activity (GIA) of the serum antibodies at 10mg/ml total purified IgG. GIA was
 39 compared between DFX and monthly-medium vaccinee serum samples 6-months after the
 40 final vaccination (**A**). A Spearman correlation analysis was performed to determine the
 41 relationship between serum anti-RH5.1 IgG and GIA (**B**). Monthly-medium $n=7$; DFX $n=11$. A
 42 comparison between groups was performed with a Mann-Whitney test. Central box lines
 43 indicate medians and whiskers denote 5th and 95th percentiles. ** $p < 0.01$.

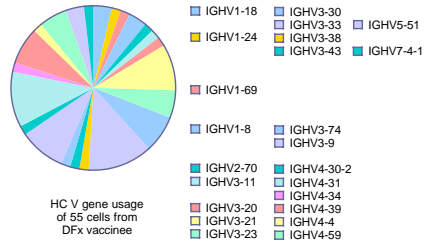
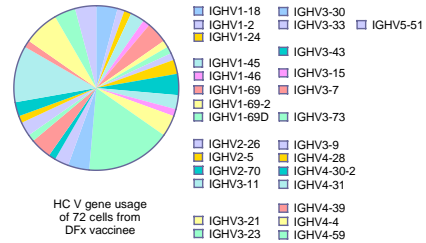
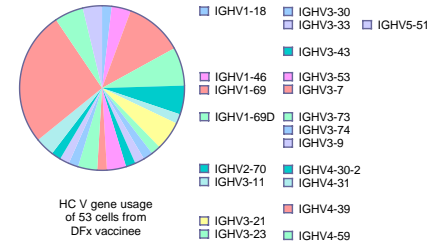
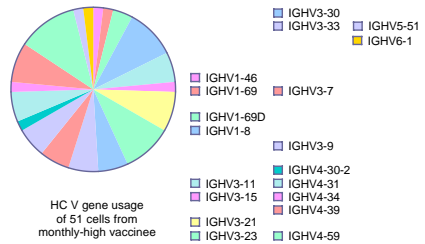
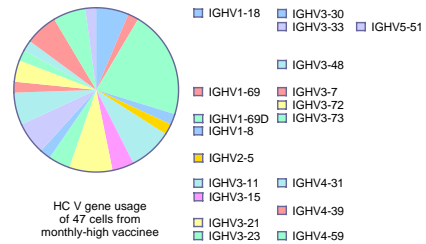
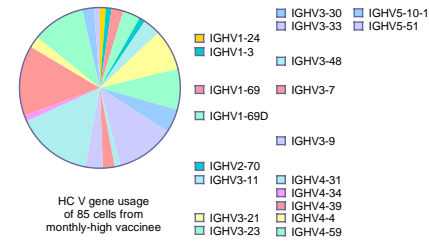
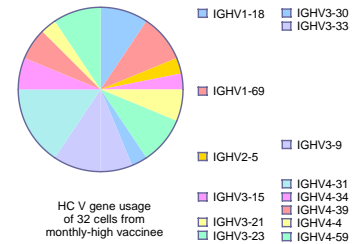
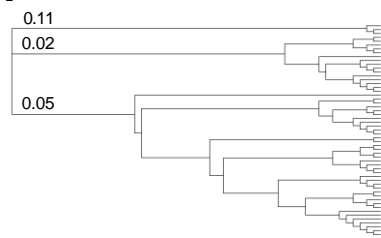
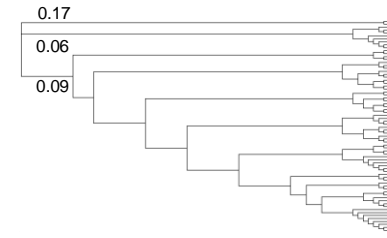
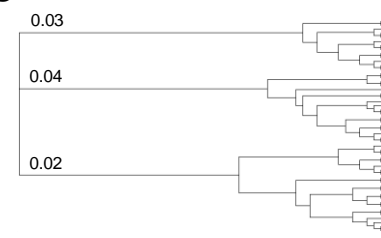
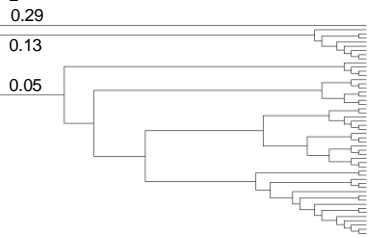
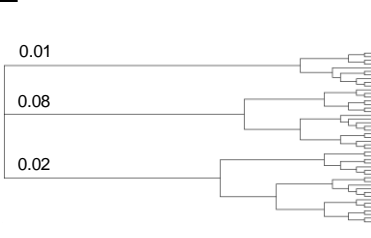
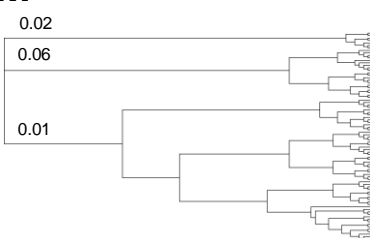
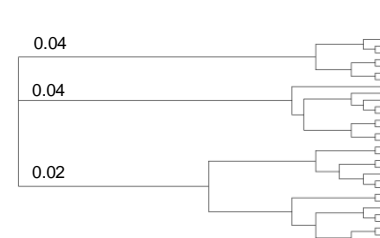


44

45 [Supplemental Figure 4. Transformed univariate systems serology parameters associated with DFx in computational](#)
 46 [modelling.](#)

47 **Relates to Figure 3.**

48 Systems serology parameters used for computational modelling were first mean-centred and variance-scaled to give Z-scored values. Seven
 49 features elevated in DFx vaccinees were subsequently identified as part of larger feature sets discriminating DFx vaccinees from monthly regimen
 50 vaccinees, or 'high' dose DFx and monthly-high vaccinees from monthly-low/ monthly-medium vaccinees: FcRn-binding (A), avidity index (B),
 51 IgG4 (C), G2S2F (D), G2S2 (E), G1FBG2 (F), and G2B (G). Monthly-low: $n=12$. Monthly-medium: $n=11$. DFx: $n=12$, Monthly-high: $n=9$. Univariate
 52 differences were assessed with Kruskal-Wallis tests with Dunn's correction for multiple comparisons. Central box lines indicate medians and
 53 whiskers denote 5th and 95th percentiles. * $p < 0.05$, ** $p < 0.01$, **** $p < 0.0001$.

A**B****C****D****E****F****G****H****I****J****K****L****M****N**

55 [Supplemental Figure 5. CDR3 VH gene usage and hierarchical clustering by vaccinee.](#)

56 **Relates to Figure 5.**

57 PBMC from pre-vaccination (Pre-vacc.), and 2-weeks post final vaccination in DFx vaccinees ($n=3$) and monthly-high vaccinees ($n=4$) were
58 enriched for B cells and then stained with phenotypic markers for single cell sorting of antigen-specific B cells defined as: live CD19+IgG+
59 lymphocytes that co-stained for monobiotinylated-PfRH5-PE and monobiotinylated-PfRH5-APC (gating strategy shown in **Supplemental Figure**
60 **1A**). Libraries were sequenced following a Smart-Seq v4 and Nextera XT pipeline on a HiSeq4000. CDR3 sequences were extracted using the
61 MiXCR pipeline including heavy chain V gene (VH) usage for DFx (**A-C**) and monthly-high vaccinees (**D-G**) by vaccinee. VH genes in >8% clones
62 per vaccinee are annotated on the pie charts. Hierarchical clustering was performed on CDR3 HC amino acid sequences and visualised as
63 dendrograms for individual DFx vaccinees (**H-J**) and monthly-high vaccinees (**K-N**) by vaccinee. Vaccinees for VH gene usage pie charts are
64 organised in same order as dendrograms, i.e. A=H, B=I, etc. The first three branches are labelled in each dendrogram with branch length (distance
65 between internal nodes) i.e. substitutions per amino acid.

Cluster	Gene	Average log2(FC)	P-adj
0	MS4A1	1.227329	5.11E-27
	YPEL5	1.107417	5.07E-20
	CD74	1.065549	4.59E-26
	DUSP2	1.040367	1.58E-05
	UCP2	1.017806	3.14E-14
1	<i>KNG1</i>	<i>1.085317</i>	<i>1.00E+00</i>
	GAREML	0.5433	1.84E-26
	PSD	0.531995	1.57E-18
	<i>RP11-217O12.1</i>	<i>0.523609</i>	<i>1.00E+00</i>
	AL162497.1	0.467258	1.40E-28
2	IRS2	0.467258	1.40E-28
	LDHA	1.351499	9.71E-09
	CCR7	1.348396	6.09E-09
	NPM1	1.326971	2.50E-13
	MIR155HG	1.303306	8.36E-11
3	ENO1	1.292817	1.43E-12
	ENO1-IT1	1.292817	1.43E-12
	MT-RNR2	1.330852	9.94E-05
	MUC3A	1.119706	9.63E-07
	<i>MT-RNR1</i>	<i>1.079884</i>	<i>1.00E+00</i>
4	KCNQ1OT1	1.054008	3.79E-11
	TAOK1	1.037066	3.86E-04
	MIR4523	1.036084	3.61E-4
	<i>IGLV2-8</i>	<i>6.83988</i>	<i>7.50E-01</i>
	<i>MIR650</i>	<i>6.83988</i>	<i>7.50E-01</i>
4	IGHG2	6.128872	1.11E-10
	RP11-731F5.2	6.128872	1.11E-10
	IGLC1	5.478077	1.26E-05
	IGLJ1	5.478077	1.26E-05
	IGLL5	5.478077	1.26E-05

66

67 [Supplemental Table 1. Top 5 differentially expressed antigen-specific B cell](#)
68 [genes per Harmonised UMAP cluster.](#)

69 **Relates to Figure 4.**

70 Top five genes shown per UMAP cluster ranked on fold change. Italics denote genes that are
71 not statistically significant following p value adjustment. Average log2(FC): average log fold
72 change between cluster and other clusters; padj: adjusted p value after correction for
73 multiplicity of testing.

Pathway	padj	NES	Leading Edge
KEGG_SYSTEMIC_LUPUS_ERYTHEMATOSUS	0.0313	2.11	HLA-DQA2, HLA-DRA, HLA-DQA1, HLA-DQB1, HLA-DOA, <u>FCGR2A</u> , <u>C7</u> , HLA-DRB5
KEGG_INTESTINAL_IMMUNE_NETWORK_FOR_IGA_PRODUCTION	0.0313	2.10	HLA-DQA2, HLA-DRA, HLA-DQA1, HLA-DQB1, HLA-DOA, <u>IL15</u> , HLA-DRB5, <u>TNFRSF17</u> , <u>ITGA4</u>
KEGG_TYPE_I_DIABETES_MELLITUS	0.0313	2.08	HLA-DQA2, HLA-DRA, HLA-DQA1, HLA-DQB1, HLA-DOA, HLA-C, HSPD1, HLA-DRB5, <u>IL1A</u> , HLA-B
KEGG_AUTOIMMUNE_THYROID_DISEASE	0.0313	2.01	HLA-DQA2, HLA-DRA, HLA-DQA1, HLA-DQB1, HLA-DOA, HLA-C, <u>CGA</u> , HLA-DRB5, HLA-B, HLA-DOB
KEGG_GRAFT_VERSUS_HOST_DISEASE	0.0464	1.97	HLA-DQA2, HLA-DRA, HLA-DQA1, HLA-DQB1, HLA-DOA, HLA-C, HLA-DRB5, <u>IL1A</u> , HLA-B
KEGG_PROTEIN_EXPORT	0.0313	1.95	<u>SEC11C</u> , <u>SPCS2</u> , <u>HSPA5</u> , <u>SRP68</u> , <u>SEC63</u> , <u>SEC61A1</u> , <u>SPCS1</u> , <u>SEC61G</u> , <u>SPCS3</u> , <u>SEC61A2</u> , <u>SEC61B</u> , <u>SRPRB</u> , <u>SRP54</u>
KEGG_ASTHMA	0.0464	1.95	HLA-DQA2, HLA-DRA, HLA-DQA1, HLA-DQB1, HLA-DOA, HLA-DRB5
KEGG_ALLOGRAFT_REJECTION	0.0313	1.94	HLA-DQA2, HLA-DRA, HLA-DQA1, HLA-DQB1, HLA-DOA, HLA-C, HLA-DRB5, HLA-B, HLA-DOB
KEGG_CELL_ADHESION_MOLECULES_CAMS	0.0313	1.92	HLA-DQA2, HLA-DRA, <u>SELPLG</u> , HLA-DQA1, HLA-DQB1, HLA-DOA, HLA-C, <u>SELL</u> , <u>ICAM2</u> , HLA-DRB5, <u>ITGA4</u> , HLA-B, HLA-DOB, <u>PTPRC</u> , <u>ITGB1</u>
KEGG_LEISHMANIA_INFECTION	0.0464	1.87	HLA-DQA2, HLA-DRA, HLA-DQA1, HLA-DQB1, HLA-DOA, <u>FCGR2A</u> , HLA-DRB5, <u>IL1A</u> , <u>ITGA4</u> , <u>NCF1</u> , <u>TLR4</u> , HLA-DOB, <u>ITGB1</u>

75

76 Supplemental Table 2. KEGG pathways enriched in monthly-high as
77 compared to DFx dosing vaccinees.

78 **Relates to Table 2.**

79 KEGG gene set enrichment analyses were run with the 5,115 significant genes from DESeq2
80 analyses comparing gene expression in PfRH5-specific CD19+IgG+ B cells from monthly and
81 DFx regimen vaccinees (top thirty genes shown in **Table 2**). All gene set pathways with
82 significant adjusted *p* value (following Benjamini-Hochberg correction for multiplicity of testing)
83 are shown, in order of enrichment. Non-HLA genes are highlighted and underlined. padj:
84 adjusted *p* value; NES: normalised enrichment score; Leading Edge: subset of genes from
85 gene set contributing most to the enrichment signal.

Pathway	p value	padj	NES	Leading Edge
HALLMARK_E2F_TARGETS	3.03E-03	6.28E-02	1.62	PAICS, RFC3, TMPO, HMGB2, CKS1B, RFC1, PTTG1, AK2, XPO1, RAD50, RACGAP1, SMC3, KPNA2, ORC6, BIRC5, TUBG1, EXOSC8, KIF2C, RAD51C, NUDT21, RAD51AP1, CCNB2, EIF2S1, CDKN3, CSE1L, ANP32E, RPA2, ORC2, CDC20, TP53, STMN1, DUT, EED, DONSON, POLD2, NBN, CDK4, PRDX4, NME1, PCNA, XRCC6, TIMELESS, BRCA1, CHEK2, MAD2L1
HALLMARK_OXIDATIVE_PHOSPHORYLATION	2.01E-03	6.28E-02	1.61	PRDX3, MRPL35, MRPL15, UQCRCQ, NNT, LDHB, LDHA, MTRF1, NDUFB7, NDUFB4, SLC25A4, SURF1, ECHS1, MRPS11, SDHC, SDHD, PDHB, ATP6V0E1, NDUFB1, ATP6V0B, TIMM8B, TIMM17A, COX15, MRPS12, SLC25A5, NDUFAB1, NDUFB6, FXN, UQCRCFS1, UQCRCR, COX7A2L, DLAT, CYC1, COX6C, MPC1, UQCRC2, ISCU, NDUFA6, ETFA, CASP7, ATP6V1E1, NDUFV2, MDH1, CYCS, COX6A1, NDUFS6, PDHA1, SDHB, NDUFS1, UQCRC1, ATP6V1G1, MRPL34, HSD17B10, ACO2, DECR1, ATP6V1H, POLR2F, UQCRB, COX5B, PHB2, MDH2, HSPA9, GOT2, AIFM1, MRPL11, TOMM22, ACADVL, GPI
HALLMARK_INTERFERON_ALPHA_RESPONSE	1.68E-02	1.68E-01	1.61	SAMD9L, TRIM5, HLA-C, CASP1, SELL, IL15, BST2, PSMB8, PSMA3, PSME1, PSME2, ISG20, UBE2L6, TAP1, B2M, EPST11, CD47, TXNIP, IFITM2, MX1, TRAFD1, LAP3, PARP14, CCRL2, SP110, ADAR, CD74, IFITM3, SLC25A28, IRF2, ELF1, IRF1, NCOA7, TDRD7, RNF31
HALLMARK_MTORC1_SIGNALING	5.03E-03	6.28E-02	1.58	SDF2L1, TP11, GLRX, PSAT1, SHMT2, P4HA1, SLC7A11, HSPA5, XBP1, GAPDH, HSPD1, PPA1, PSMA3, USO1, LDHA, LTA4H, EDEM1, RAB1A, TUBG1, PSMC2, M6PR, SSR1, PDK1, HSP90B1, UFM1, EBP, CACYBP, CANX, ENO1, EIF2S2, ADD3, RPN1, BTG2, SKAP2, ALDOA, TES, BUB1, CYB5B, SLA, SEC11A, PSMC6, SC5D, LGMN, PGM1, SERP1, PSMD12, PGK1, BHLHE40, NUFIP1, PSMD13, FKBP2, TCEA1, GMPS, HSPE1, TUBA4A, CD9, ACTR3, PSMA4, PSMD14, CORO1A, NMT1, HSPA4, ITGB2, PSMB5, HSPA9, PSPH, CCT6A, CALR, YKT6, STIP1, GPI, ETF1, TFRC, ASNS, UCHL5, PHGDH, HPRT1, PSMC4, CCNG1, HMGR
HALLMARK_MYC_TARGETS_V1	4.02E-03	6.28E-02	1.56	PHB, PRDX3, HSPD1, LDHA, XPO1, TCP1, KPNA2, IMPDH2, CCT5, PSMD7, RRM1, CANX, EIF2S2, SRM, VBP1, SSBP1, CCT3, EIF2S1, NHP2, CDK2, ORC2, CDC20, APEX1, SF3A1, NDUFAB1, DUT, PSMC6, PSMB2, NPM1, POLD2, HNRNPC, CDK4, SF3B3, GNL3, RFC4, CYC1, PRDX4, PGK1, NME1, KPNB1, PTGES3, BUB3, PCNA, EIF3J, HNRNPA2B1, HSPE1, XRCC6, SSB, RNPS1, PSMA4, MAD2L1, PSMD14, PSMD1, CCT7, RPLP0, HNRNPD, TARDBP, SNRPD2, SMARCC1, EIF4H, PHB2, PSMA7, CCT2, GOT2, CNBP, PPM1G, FBL, ETF1, RPS2, CBX3, HPRT1, HNRNPR, PSMC4, HSP90AB1, MRPL23, TUFM, SNRPD3, PSMD8
HALLMARK_UNFOLDED_PROTEIN_RESPONSE	2.97E-02	2.48E-01	1.50	PSAT1, CKS1B, HSPA5, FKBP14, XBP1, EXOSC1, DNAJC3, DNAJB9, SPCS1, EDEM1, HERPUD1, SPCS3, SSR1, PDIA6, GOSR2, EIF4EBP1, SRPRB, HSP90B1, TTC37, EIF2S1, NHP2, PDIA5, EIF4A2, ALDH18A1, SEC11A, NPM1, SERP1, WIP1, EIF4A3, CXXC1, PREB, PAIP1, TSPYL2, YWHAZ, EXOSC5, DCP2, ATF4, HSPA9, CALR, SLC30A5, NFYB
HALLMARK_PROTEIN_SECRETION	4.38E-02	3.07E-01	1.47	LMAN1, BET1, SNX2, USO1, SEC24D, VPS45, TMED10, SNAP23, RAB14, M6PR, NAPA, RAB2A, COPB2, GOSR2, AP2B1, STX7, COPE, TMED2, RAB9A, ARCN1, ANP32E, PPT1, TMX1

86

87

Supplemental Table 3. HALLMARK pathways enriched in monthly-high as compared to DFx dosing vaccinees.

88

Relates to Table 2

89

Hallmark gene set enrichment analyses were run with the 5,115 significant genes from DESeq2 analyses comparing gene expression in PfrH5-specific CD19+IgG+ B cells from monthly-high and DFx regimen vaccinees (top thirty genes shown in **Table 2**). All gene set pathways with significant adjusted *p* values (following Benjamini-Hochberg correction for multiplicity of testing) are shown in order of enrichment. padj: adjusted *p* value; NES: normalised enrichment score; Leading Edge: subset of genes from gene set contributing most to the enrichment signal.

90

91

92

Supplemental Systems Serology Methods

Fluorescent Primary and Secondary Antibodies

The following fluorescent antibodies were purchased from BD Biosciences: anti-human CD14-APC-Cy7 (557831), anti-human CD56-PE-Cy7 (335791), and anti-human MIP1 β -BV421 (562900). Additional fluorescent antibodies were purchased from BioLegend: anti-human CD66b-PacificBlue (305112), anti-human CD3-APC-Cy7 (300426), anti-human CD3-BV785 (300472), anti-human CD107a-BV605 (328634), and anti-human IFN γ -PE (506507). A FITC-conjugated, goat anti-guinea pig complement C3 polyclonal antibody was purchased from MP Biomedical (0855385). PE-conjugated secondary antibodies were purchased from Southern Biotech for the detection of total human IgG (9040-09), IgM (9020-09), IgA1 (9130-09), IgA2 (9140-09), IgG1 (9052-09), IgG2 (9070-09), IgG3 (9210-09), and IgG4 (9200-09).

Antigen Coupling to Fluorescent Beads

NeutrAvidin-labelled yellow-green (F8776) and red (F8775) fluorescent 1 μ m microspheres were purchased from Thermo Fisher Scientific. For immune functional assays, 1.8x10⁸ NeutrAvidin-labelled fluorescent microspheres were coupled to 5 μ g monobiotinylated PfrH5 antigen (exact construct as described above in flow cytometry section and (2)) by co-incubation in PBS/5% BSA (PBSA) overnight at 4°C, then the beads were washed twice with PBSA. Magplex-C microspheres (Luminex Corp) were covalently coupled to streptavidin (016-000-113, Jackson Immunoresearch) using a two-step carbodiimide reaction. Magplex-C beads (9x10⁸) were washed, resuspended in 100mM NaH₂PO₄ (pH6.2), and activated by incubating with 500 μ g Sulfo-NHS (A39269, Pierce) and 500 μ g EDC (A35391, Pierce) for 30 min at room temperature (RT). The beads were washed three times with coupling buffer (50mM MES, pH 5.0), then incubated with streptavidin in 500 μ L of coupling buffer for 2h at RT. The beads were washed with PBS/0.05% Tween-20, incubated overnight at 4°C with 100 μ g/mL monobiotinylated PfrH5 in PBSA, washed, and stored in PBS/0.05% sodium azide.

THP-1 Monocyte Phagocytosis Assay

An assay for measuring antibody-dependent THP-1 monocyte / cellular phagocytosis (ADCP) was used as previously described (4). Briefly, 1 μ m yellow-green fluorescent NeutrAvidin beads were coupled to monobiotinylated PfrH5 antigen and blocked overnight with PBSA. The beads were then washed twice with PBSA, diluted to 1.8x10⁸ beads/mL, and 10 μ L beads/well were added to a 96-well round-bottom microplate. Diluted plasma from immunised subjects (10 μ L/well) was added to the beads and incubated at 37°C for 2h to allow the formation of immune complexes. Unbound antibodies were washed off, then 25,000 THP-1 cells/well (TIB202, ATCC) were added to the beads in 200 μ L THP-1 medium (R10 + 55 mM β -ME) and incubated overnight at 37°C. Cells were fixed and acquired on an Intellicyt iQue Screener PLUS flow cytometer. The phagocytic score for each sample was calculated as (% bead-positive cells) x (geometric median fluorescence intensity [gMFI] of bead-positive cells) / (10 x gMFI of first bead-positive peak).

Primary Neutrophil Phagocytosis Assay

An assay for measuring antibody-dependent neutrophil phagocytosis (ADNP) has been described previously (5). Briefly, 1 μ m yellow-green fluorescent NeutrAvidin beads were coupled to monobiotinylated PfrH5 antigen and blocked with PBSA overnight at 4°C. The beads were then washed twice with PBSA and diluted to 1.8x10⁸ beads/mL. PfrH5-coupled beads (10 μ L/well) and diluted test plasma (10 μ L/well) were combined in a round-bottom 96-well plate, then incubated at 37°C for 2h. Primary leucocytes were isolated from freshly drawn whole blood (collected from healthy donors in anticoagulant citrate dextrose tubes) by treatment with ACK red blood cell lysis buffer, then diluted in R10 media to 250,000 cells/mL. After immune complex formation, the beads were washed, combined with 50,000 primary leucocytes/well, and incubated for 1h at 37°C. Cells were stained for surface CD66b, CD14,

146 and CD3, fixed, and acquired on an Intellicyt iQue Screener PLUS flow cytometer. Gates were
147 drawn to identify singlet SSC^{hi}CD66b+CD14-CD3- cells, and phagocytic scores for each
148 sample were calculated as (% bead-positive cells) x (gMFI of bead-positive cells) / (10 x gMFI
149 of the first bead-positive peak).

150

151 *Complement Deposition Assay*

152 An assay for measuring antibody-dependent complement deposition (ADCD) was used as
153 previously described (6). Briefly, 1mm red fluorescent NeutrAvidin beads were incubated with
154 monobiotinylated PfrH5 antigen, blocked with PBSA, then washed and diluted to 1.8x10⁸
155 beads/mL. PfrH5-coupled beads (10µL/well) were combined with diluted test plasma
156 (10µL/well) in a 96-well round-bottom microplate, then incubated at 37°C for 2h. Guinea pig
157 complement (CL4051, CedarLane) was diluted in gelatin veronal buffer containing calcium
158 and magnesium (GVB++; IBB-300, Boston Bioproducts). The beads were washed with PBS
159 and incubated with diluted complement for 20 min at 37°C. The beads were then washed with
160 5mM EDTA, stained with FITC-conjugated anti-complement C3, and acquired on an Intellicyt
161 iQue Screener PLUS flow cytometer. Gates were drawn on singlet, red fluorescent particles,
162 and complement deposition was reported as the median FITC fluorescence intensity.

163

164 *NK cell Activation Assay*

165 An assay for measuring antibody-dependent NK cell activation (ADNKA) has been described
166 previously (7, 8). Flat-bottom 96-well ELISA plates (439454, Thermo Fisher) were coated with
167 monobiotinylated PfrH5 antigen, then blocked with PBSA. Plasma samples from test subjects
168 were diluted in PBSA, added to the plates, and incubated for 2h at 37°C. Primary human NK
169 cells were purified from buffy coats from healthy donors using the RosetteSep human NK cell
170 enrichment cocktail (15065, StemCell), then resuspended in R10 media containing 10µg/mL
171 brefeldin A (B7651, Sigma), GolgiStop (554724, BD Biosciences), and fluorescent anti-human
172 CD107a. The ELISA plates were washed three times with PBS, then isolated NK cells
173 (25,000/well) were added and incubated at 37°C for 5h. The cells were then stained for surface
174 CD56 and CD3, permeabilised, stained with fluorescent antibodies to IFNγ and MIP1β, fixed,
175 and acquired on an Intellicyt iQue Screener PLUS flow cytometer. Gates were drawn on
176 singlet, CD56+/CD3- cells, and results were reported as the percentages of these cells that
177 expressed surface CD107a, intracellular MIP1β, or intracellular IFNγ.

178

179 *Antibody Isotype and Subclass Analysis*

180 The isotypes and subclasses of PfrH5 antigen-specific antibodies were quantified using a
181 previously described method (9). Magplex-C microspheres were coupled to streptavidin via
182 carbodiimide crosslinking with Sulfo-NHS and EDC. Streptavidin-coupled beads were then
183 incubated overnight with monobiotinylated PfrH5 antigen, blocked with PBSA, and added to
184 black flat-bottom 384-well plates (781906, Greiner BioOne) so that each well contained 1500
185 PfrH5-coupled beads. Plasma from test subjects was diluted in PBSA and co-incubated with
186 the beads for 2h at RT on a plate shaker (800rpm). The beads were then washed and
187 incubated with a PE-conjugated antibody to detect total human IgG, hulgG1, hulgG2, hulgG3,
188 hulgG4, hulgM, hulgA1, or hulgA2 for 1h at RT on a plate shaker (800rpm). To evaluate anti-
189 PfrH5 IgG avidity, samples were incubated with or without 7M urea prior to incubation with
190 total human IgG antibody. The beads were then washed and acquired on an Intellicyt iQue
191 Screener PLUS flow cytometer. Results for all 9 parameters were reported as the median PE
192 fluorescence intensity. For the avidity assay, an avidity index is reported as (MFI with urea
193 incubation) / (MFI without urea incubation). To note, previously published data on anti-PfrH5
194 IgG avidity was generated using a sodium thiocyanate chemical displacement ELISA with
195 post-vaccination sera samples (3).

196

197 *Fc-binding Protein Array*

198 The binding of PfrH5 antigen-specific antibodies to human Fc receptors (FcR) and
199 complement C1q was measured using a previously-described assay (10, 11). Briefly, avi-

200 tagged FCGR2A-H, FCGR2A-R, FCGR2B, FCGR3A-F, FCGR3A-V, FCGR3B, FcRn, and
201 FcαR proteins were produced and purified by the Duke Human Vaccine Institute Protein
202 Production Facility. These proteins were then biotinylated with BirA ligase using a
203 commercially available kit (BirA500, Avidity). Purified human C1q protein (C1740, Sigma) was
204 biotinylated using EZ-Link Sulfo-NHS-LC-LC-Biotin (A35358, Pierce) according to the
205 manufacturer's instructions. These biotinylated Fc domain-binding proteins were then
206 incubated with streptavidin-PE (PJ31S, Prozyme) to generate the assay detection reagents.
207 Magplex-C microspheres were coupled to monobiotinylated PfrH5 antigen as described
208 above, blocked with PBSA, and added to 384-well plates so that each well contained 1500
209 PfrH5-coupled beads. Plasma from test subjects was diluted in PBSA, added to the beads,
210 and incubated for 2h at RT on a plate shaker (800rpm). The beads were then washed,
211 incubated with one of the PE/FcR conjugates for 1h at RT on a plate shaker (800rpm), washed
212 again, and acquired on an Intellicyt iQue Screener PLUS flow cytometer. Results for all 9
213 parameters were reported as the median PE fluorescence intensity.
214

215 *Fc glycan Analysis*

216 The Fc glycans on PfrH5 antigen-specific IgG were analysed using a previously described
217 method (12, 13). Briefly, 200µL of plasma from each vaccinated subject was heat-inactivated
218 at 56°C for 1h, then centrifuged at 20,000xg for 10min at RT. The resulting supernatant
219 samples were first pre-cleared by incubating with 1mm magnetic streptavidin-coated
220 microspheres (S1420S, New England Biolabs) for 1h at RT. A magnet was used to pellet the
221 beads, and the supernatants were then transferred to new tubes containing streptavidin-
222 coated beads that had been coupled to monobiotinylated PfrH5 antigen. The PfrH5-coupled
223 beads were incubated with plasma samples for 1h at 37°C, then washed and incubated with
224 IdeZ enzyme (P0770S, New England Biolabs) for 1h at 37°C to remove the Fc fragments from
225 the bead-bound antibodies. These Fc fragments were transferred to new tubes and incubated
226 with PNGase F (A28404, Applied Biosystems) for 1h at 50°C to remove the glycans. The
227 glycans were then isolated and labelled with APTS dye using a GlycanAssure kit (A28676,
228 Thermo Fisher) according to the manufacturer's instructions. Finally, APTS-labelled glycan
229 samples were analysed by capillary electrophoresis on an ABI 3500xL Genetic Analyzer. The
230 area under the peak for each Fc glycan structure was calculated using GlycanAssure data
231 analysis software. Results were then reported as the frequency (%) of each glycan structure
232 within a given sample. A total of 25 glycan structures were measured, of which 11 were
233 detectable in >50% vaccinees and included in downstream analyses: G2S2, G2S2F, G1S1F,
234 G2S1F, G0F, G1F, G1.F-G1FB, G1.FB-G2, G2B, G2F, and G2FB.

235 **References**

- 236 1. Payne RO, Silk SE, Elias SC, Miura K, Diouf A, Galaway F, et al. Human vaccination
237 against RH5 induces neutralizing antimalarial antibodies that inhibit RH5 invasion complex
238 interactions. *JCI Insight*. 2017;2(21).
- 239 2. Nielsen CM, Ogbe A, Pedroza-Pacheco I, Doeleman SE, Chen Y, Silk SE, et al.
240 Protein/AS01B vaccination elicits stronger, more Th2-skewed antigen-specific human T
241 follicular helper cell responses than heterologous viral vectors. *Cell Rep Med*.
242 2021;2(3):100207.
- 243 3. Minassian AM, Silk SE, Barrett JR, Nielsen CM, Miura K, Diouf A, et al. Reduced
244 blood-stage malaria growth and immune correlates in humans following RH5 vaccination.
245 *Med (N Y)*. 2021;2(6):701-19 e19.
- 246 4. Ackerman ME, Moldt B, Wyatt RT, Dugast AS, McAndrew E, Tsoukas S, et al. A
247 robust, high-throughput assay to determine the phagocytic activity of clinical antibody
248 samples. *J Immunol Methods*. 2011;366(1-2):8-19.
- 249 5. Karsten CB, Mehta N, Shin SA, Diefenbach TJ, Slein MD, Karpinski W, et al. A
250 versatile high-throughput assay to characterize antibody-mediated neutrophil phagocytosis.
251 *J Immunol Methods*. 2019;471:46-56.
- 252 6. Fischinger S, Fallon JK, Michell AR, Broge T, Suscovich TJ, Streeck H, et al. A high-
253 throughput, bead-based, antigen-specific assay to assess the ability of antibodies to induce
254 complement activation. *J Immunol Methods*. 2019;473:112630.
- 255 7. Jegaskanda S, Job ER, Kramski M, Laurie K, Isitman G, de Rose R, et al. Cross-
256 reactive influenza-specific antibody-dependent cellular cytotoxicity antibodies in the absence
257 of neutralizing antibodies. *J Immunol*. 2013;190(4):1837-48.
- 258 8. Lu LL, Chung AW, Rosebrock TR, Ghebremichael M, Yu WH, Grace PS, et al. A
259 Functional Role for Antibodies in Tuberculosis. *Cell*. 2016;167(2):433-43 e14.
- 260 9. Brown EP, Licht AF, Dugast AS, Choi I, Bailey-Kellogg C, Alter G, et al. High-
261 throughput, multiplexed IgG subclassing of antigen-specific antibodies from clinical samples.
262 *J Immunol Methods*. 2012;386(1-2):117-23.
- 263 10. Brown EP, Dowell KG, Boesch AW, Normandin E, Mahan AE, Chu T, et al.
264 Multiplexed Fc array for evaluation of antigen-specific antibody effector profiles. *J Immunol*
265 *Methods*. 2017;443:33-44.
- 266 11. Brown EP, Weiner JA, Lin S, Natarajan H, Normandin E, Barouch DH, et al.
267 Optimization and qualification of an Fc Array assay for assessments of antibodies against
268 HIV-1/SIV. *J Immunol Methods*. 2018;455:24-33.
- 269 12. Mahan AE, Tedesco J, Dionne K, Baruah K, Cheng HD, De Jager PL, et al. A
270 method for high-throughput, sensitive analysis of IgG Fc and Fab glycosylation by capillary
271 electrophoresis. *J Immunol Methods*. 2015;417:34-44.
- 272 13. Brown EP, Normandin E, Osei-Owusu NY, Mahan AE, Chan YN, Lai JI, et al.
273 Microscale purification of antigen-specific antibodies. *J Immunol Methods*. 2015;425:27-36.